AIAA 2001−0476

Direct Calculations of Two- and Three- Dimensional Detonations by an Extended CE/SE Method

Zeng-Chan Zhang[1] **S.T. John Yu**[2] **Hao He**[3]
Wayne State University
Detroit, Michigan 48202

Sin-Chung Chang[4]
NASA Glenn Research Center
Cleveland, Ohio 44135

Abstract

The present paper reports the two- and three-dimensional calculations of propagating detonation waves by the modified space-time CE/SE method, which is based on quads and hexes for two and three dimensional meshes. The Euler equations in conjunction with a species equation are solved in a time-accurate manner. The chemical reaction is modeled by a one-step Arrhenius kinetics. The stiff source term is treated by a volumetric integration over a space-time region. As in the original space-time CE/SE method, the present approach does not use the Riemann solver and the associated directional splitting. Therefore, the logic and operation count is significantly simpler. The present method is successfully applied to solve two- and three-dimensional propagating detonations. All salient flow features of detonations are crisply resolved. The modified CE/SE method is indeed a viable approach for unsteady detonation waves.

1. Introduction

Detonation wave was first recognized by Mallard and Le Chatelier during their studies of flame propagation. The research of detonation waves was pioneered by Zeldovich, von Neumann, and Doering, i.e., the ZND model [3], in which a steady detonation wave consisting of an non-reacting flow shock followed by a finite-rate reaction zone is postulated. This important insight provided preliminary knowledge of detonations. However, further experimental evidences showed that detonation waves are often unstable with transverse wave structure, and the unsteady pressure spike is much higher than that predicted by the ZND model.

The calculation of stable and unstable detonation waves is a great challenge for any computational fluid dynamics (CFD) method. To date, various numerical methods have been applied to detonations [2-14]. In our previous works [25,26], one- and two-dimensional stable and unstable detonations have been calculated using the space-time CE/SE method.

Originally developed by Chang and coworkers, the CE/SE method [15-19] is a new numerical framework for conservation laws. The CE/SE method differs substantially from other well-established methods, and has many non-traditional features, including a unified treatment of space and time, the introduction of conservation element (CE) and solution element (SE), and a novel shock capturing strategy without using Rieman solvers. Moreover, triangles and tetrahedrons are used and the method is naturally suited for unstructured meshes.

For structured meshes, Zhang et al [20,21,23] developed an extension of the CE/SE method for quad and hexes in two-and three spatial dimensions. In this extended CE/SE method, a single CE at each grid point is employed for solving conservation laws in one, two, and three spatial dimensions, instead of two in one-dimensional, three in two-dimensional, and four in three-dimensional problems in the original CE/SE method. Here, the CE is used to calculate flow variables only, whilst the gradients of flow variables are calculated by a central-differencing reconstruction procedure. For equations in one spatial dimension, this approach is a special case of Chang's a-ε scheme. For problems in two and three spatial dimensions, the present method can be easily applied to a regular structured mesh. Nevertheless, this modified scheme inherits most of the advantageous features of the original CE/SE method, including efficient operational count, easiness of implementing non-reflective boundary condition, and high-fidelity resolution of wave motions. In particular, the use of

[1]Research Associate. AIAA Member, Email: zczhang@me1.eng.wayne.edu
[2]Associate Professor, AIAA Member, Email: styu@me1.eng.wayne.edu
[3]Ph.D. student, Email: haohe@me1.eng.wayne.edu
[4]Senior Aerospace Engineer, Email: sin-chung,chang@lerc.nasa.gov

Riemann solvers (the paradigm of modern upwind schemes) is excluded. Therefore, the computational logic is considerably simpler. In this paper, we apply the modified CE/SE method to the two- and three-dimensional propagating detonation waves.

The rest of this paper is organized as follows. In Section 2, a brief account of 3D theoretical model of the detonation is provided. For completeness, the classical ZND theoretical solution is provided in section 3. In Section 4, the modified space-time CE/SE method for two- and three-dimensional case is reviewed. In Section 5, numerical solutions will be reported, including (1) two-dimensional unsteady waves with periodic boundary condition, (2) detonation propagation in a thrust tube with wavy walls, and (3) three-dimensional unsteady detonations. We then offer concluding remarks and provide cited references.

2. Theoretical Model

The governing equation of detonating flows in three-spatial dimensions can be formulated by the Euler equations coupled with a species equation:

$$\frac{\partial u_m}{\partial t}+\frac{\partial f_m}{\partial x}+\frac{\partial g_m}{\partial y}+\frac{\partial q_m}{\partial z}=\mu_m \qquad (2.1)$$

where $m=1, 2, 3, 4, 5,$ and 6 for the continuity, three moment, the energy, and the species equations, respectively. The vector $[u_m]$ is the unknown, $[f_m]$, $[g_m]$ and $[q_m]$ are flux vectors, and $[\mu_m]$ is the source term:

$$[u_m]=\begin{pmatrix}\rho\\ \rho u\\ \rho v\\ \rho w\\ \rho E\\ \rho Z\end{pmatrix},\quad [\mu_m]=\begin{pmatrix}0\\ 0\\ 0\\ 0\\ 0\\ \dot{\omega}\end{pmatrix},\quad [f_m]=\begin{pmatrix}\rho u\\ \rho u^2+p\\ \rho uv\\ \rho uw\\ (\rho E+p)u\\ \rho uZ\end{pmatrix}$$

$$[g_m]=\begin{pmatrix}\rho v\\ \rho uv\\ \rho v^2+p\\ \rho vw\\ (\rho E+p)v\\ \rho vZ\end{pmatrix},\quad [q_m]=\begin{pmatrix}\rho w\\ \rho wu\\ \rho wv\\ \rho w^2+p\\ (\rho E+p)w\\ \rho wZ\end{pmatrix} \qquad (2.2)$$

Here, ρ is density, u, v and w are the x-, y- and z-components of velocity, p is pressure, Z is the mass fraction of the reactant, and $E= e + Zq_o + (u^2+v^2+w^2)/2$ is the total energy with e as the internal energy and q_o as the heat release due to the chemical reaction. In the species equation, a source term exists due to a one-step, irreversible chemical reaction, which is modeled by finite-rate kinetics. This source term is expressed as

$$\dot{\omega}=-K\rho Z\exp(-E^+/R_uT) \qquad (2.3)$$

where K is the pre-exponential factor of the Arrhenius kinetics, E^+ is the activation energy, and R_u is the universal gas constant. We assume that the fluid is polytropic, i.e., the molecular weights and the specific heats are constants for the unburned and the burned gases.

To proceed, the above equations are non-dimensionalized based on the state of the unburned gas, e.g., ρ_0, p_0, T_0, which are density, pressure, and temperature of the unburned state, respectively. A reference velocity is defined as $\sqrt{RT_o}$, which is similar to the speed of the sound of the unburned gas, and $R=R_u/M_w$, M_w is the molecular weight of unburned gas. The reference length x_0 is chosen as the half- reaction length, $L_{1/2}$, which is defined as the distance between the detonation front and the point, where half of the reactant is consumed by combustion. To be consistent, the total energy E, internal energy e, and heat release are non-dimensionalized by RT_o. The non-dimensional variables are defined as follows:

$$\bar{x}=\frac{x}{x_0},\quad \bar{\rho}=\frac{\rho}{\rho_0},\quad \bar{p}=\frac{p}{p_0},\quad \bar{T}=\frac{T}{T_0}, \qquad (2.4a)$$

$$\bar{u}=\frac{u}{\sqrt{RT_0}},\quad \bar{v}=\frac{v}{\sqrt{RT_0}},\quad \bar{w}=\frac{w}{\sqrt{RT_0}}, \qquad (2.4b)$$

$$\bar{t}=\frac{t}{x_0/\sqrt{RT_0}},\quad \bar{K}=\frac{K}{\sqrt{RT_0}} \qquad (2.4c)$$

$$\bar{E}=\frac{E}{RT_0},\quad \bar{E}^+=\frac{E^+}{R_uT_0},\quad \bar{q}_0=\frac{q_0}{RT_0}, \qquad (2.4d)$$

where the subscript '0' denotes the unburned state. Using the above non-dimensionalied variables, we can obtain the same equation as that of Eq. (2.1) with one exception in the source term $\dot{\omega}$.

$$\bar{\dot{\omega}}=-\bar{K}x_0\bar{\rho}Z\exp(-\bar{E}^+/\bar{T}) \qquad (2.5)$$

Where x_0 is added to the expression. For convenience, we will drop the bar above each variable in the following discussions. Thus, Eq. (2.5) becomes

$$\dot{\omega} = -Kx_0 \rho Z \exp(-E^+ / T) \qquad (2.5)'$$

3. ZND Analytical Solution

To fully control the growth of the instability waves, we need to use one-dimensional analytical solutions as the initial conditions in our two- and three-dimensional calculations. For completeness, a brief review of the classical ZND solution is provided in this section.

Consider the one-dimensional reactive Euler equations:

$$\frac{\partial u_m}{\partial t} + \frac{\partial f_m}{\partial x} = \mu_m \qquad (3.1)$$

where

$$[u_m] = \begin{pmatrix} \rho \\ \rho u \\ \rho E \\ \rho Z \end{pmatrix}, [f_m] = \begin{pmatrix} \rho u \\ \rho u^2 + p \\ (\rho E + p)u \\ \rho u Z \end{pmatrix}, [\mu_m] = \begin{pmatrix} 0 \\ 0 \\ 0 \\ \dot{\omega} \end{pmatrix} \qquad (3.2)$$

We assume that the detonation wave propagates at a constant velocity D. We then transform the coordinates such that the spatial origin is on the shock wave. The equations of this steady problem in the new coordinate system become

$$\frac{d}{dx}(\rho u) = 0 \qquad (3.3a)$$

$$\frac{d}{dx}(\rho u^2 + p) = 0 \qquad (3.3b)$$

$$\frac{d}{dx}[(\rho E + p)u] = 0 \qquad (3.3c)$$

$$\frac{d}{dx}(\rho u Z) = \dot{\omega} \qquad (3.3d)$$

According to the non-dimensional variables defined in Eq. (2.4), we have the following non-dimensional parameters in the unburned gas:

$$\rho=1, \quad p=1, \quad T=1 \text{ and } \quad u = -D \qquad (3.4)$$

By using Eqs. (3.3a-c) in conjunction with the conditions in Eq. (3.4), we have the flow variables in the flame zone as

$$\rho u = -D \qquad (3.5)$$

$$\rho u^2 + p = D^2 + 1 \qquad (3.6)$$

$$\rho u\left(\frac{1}{\gamma-1}\frac{p}{\rho} - q_0\lambda + \frac{u^2}{2}\right) + pu = -D\left(\frac{\gamma}{\gamma-1} + \frac{D^2}{2}\right) \qquad (3.7)$$

Where the mass fraction of the product $\lambda = 1-Z$. Eqs. (3.5-6) can be rewritten as:

$$\rho = -D/u \qquad (3.8)$$

$$p = Du + D^2 + 1 \qquad (3.9)$$

Substituting Eqs. (3.8) and (3.9) into Eq. (3.7), we obtain

$$\frac{1}{2}u^2 + \frac{\gamma}{\gamma+1}\left(D + \frac{1}{D}\right)u + \frac{\gamma-1}{\gamma+1}\left(q_0\lambda + \frac{\gamma}{\gamma-1} + \frac{D^2}{2}\right) = 0 \qquad (3.10)$$

Equation (3.10) is a second-order polynomial of u and its solution is

$$u = -\frac{\gamma}{\gamma+1}\left(D + \frac{1}{D}\right) + \sqrt{\xi(\lambda)} \qquad (3.11)$$

where

$$\xi(\lambda) = \left[\frac{\gamma}{\gamma+1}\left(D + \frac{1}{D}\right)\right]^2 - 2\frac{\gamma-1}{\gamma+1}\left(q_0\lambda + \frac{\gamma}{\gamma-1} + \frac{D^2}{2}\right) \qquad (3.12)$$

Note that Eq. (3.10) has two roots. The solution presented in (3.11) is chosen. The other solution does not exist in most real situations. Let $\xi(\lambda) = 0$ in Eq. (3.12), i.e., enforcing identical roots for Eq. (3.10), the upper Chapman-Jouguet (C-J) velocity is obtained,

$$D_{C-J}^2 = [\gamma + (\gamma^2 - 1)q_0] + \sqrt{[\gamma + (\gamma^2 - 1)q_0]^2 - \gamma^2} \qquad (3.13)$$

Note that, the above C-J velocity can also be obtained by assuming that the Rayleigh line and the Hugoniot curve have one and only one intersecting (tangent) point.

By using Eq. (3.13), we can get the C-J velocity $D_{C\text{-}J}$ if γ and q_0 is given. We can then define the detonation wave velocity (D) by introducing the overdriven factor f :

$$D^2 = fD_{C-J}^2 \tag{3.14}$$

By specifying a value of f, the detonation velocity D is determined. As a result, we can calculate u, ρ and p corresponding to the values of λ by Eqs. (3.11), (3.8) and (3.9), respectively.

To proceed, we substitute Eq. (3.3a) into Eq. (3.3d) for the relation between λ and x, and we get

$$\frac{d\lambda}{dx} = Kx_0 \frac{1-\lambda}{u} \exp[-E^+ / T] \tag{3.15}$$

We can integrate Eq. (3.15) by standard numerical methods to obtain the λ value at each grid point.

To recap, the analytical solution of the one dimensional ZND detonation wave can be calculated by Eqs. (3.8,9) and (3.11-15). A typical ZND detonation wave solution, specified by the following flow conditions in (3.13), is shown in Fig. 3.1.

$$q_0 = 50, \quad E^+ = 50, \quad \gamma = 1.2, \quad f = 1.6 \tag{3.16}$$

Because both flow variables and their spatial derivatives are used as the unknowns and solved simultaneously in the CE/SE method, we need the spatial derivatives of the flow variables as part of the initial condition. The x-derivatives of the flow variables can be calculated by applying the chain rule to Eqs. (3.8,9), (3.11,12) and (3.15). For example, by using Eqs. (3.11,12), we can get

$$\frac{du}{dx} = -(\frac{\gamma-1}{\gamma+1} q_0) / \sqrt{\xi(\lambda)} \frac{d\lambda}{dx} \tag{3.17}$$

where $d\lambda/dx$ is calculated by Eq. (3.15). After du/dx is obtained, we can get other derivatives by using Eqs. (3.8, 9):

$$\frac{d\rho}{dx} = \frac{D}{u^2} \frac{du}{dx} \tag{3.18}$$

$$\frac{dp}{dx} = D \frac{du}{dx} \tag{3.19}$$

Finally, by using Eqs. (3.17-19), each U_{mx}, for $m = 1$, 2, 3, and 4, can be calculated. This concludes the discussions of the analytical solutions of the ZND detonation waves.

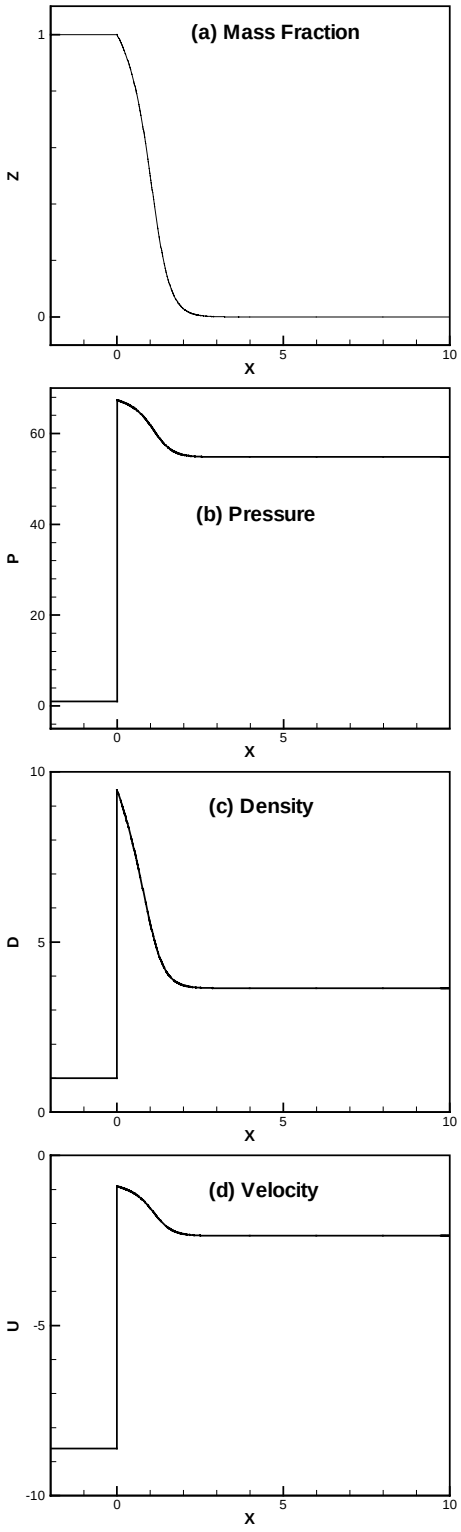

Fig. 3.1 Analytical solution profiles of an one-dimensional ZND detonation wave: (a) mass fraction; (b) pressure; (c) density, and (d) velocity.

4. Modified Space-Time CE/SE Method

The details about the modified Space-Time CE/SE method can be found in [20-23]. For completeness, a brief discussion of this extended CE/SE method is provided. First, we consider the two-dimensional equation:

$$\frac{\partial u_m}{\partial t}+\frac{\partial f_m}{\partial x}+\frac{\partial g_m}{\partial y}=\mu_m \qquad (4.1)$$

Let $x_1 = x$, $x_2 = y$ and $x_3 = t$ be the coordinates of a three-dimensional Euclidean space E_3. By using Gauss' divergence theorem in E_3, it can be shown that Eq. (4.1) is equivalent to the following integral equations:

$$\oint_{S(V)} \vec{h}_m \cdot d\vec{S} = \int_V \mu_m dV \qquad (4.2)$$

Here $\vec{h}_m = (u_m,\ f_m,\ g_m)$, $S(V)$ is the boundary of an arbitrary space-time region V in E_3. And $\vec{h}_m \cdot d\vec{S}$ is the space-time flux $\vec{h}_m$ leaving the region V through the surface element $d\vec{S}$.

In two spatial dimensions, quadrilateral is used as the basic element in the modified CE/SE method for space-time integration. Refer to Fig. 4.1. The grid point is located at the center (square symbols) of each quadrilateral. Contrast to the original CE/SE method, only one conservation element (CE) and one solution element (SE) are needed in each grid point.

Due to the stiff source term in Eq. (2.1), a locally implicit treatment [24] is employed. Thus, the definition of SE is slightly different from the one defined in [20-23]. Associated with point Q, the SE is defined as the union of (i) interior of the polygon cylinder $A_1B_1A_2B_2A_3B_3A_4B_4A_1'B_1'A_2'B_2'A_3'B_3'A_4'B_4'$, (ii) horizontal mid plane $A_1B_1A_2B_2\ A_3B_3A_4B_4$, and (iii) four lateral planes $QQ''B_1''B_1$, $QQ''B_2''B_2$, $QQ''B_3''B_3$, $QQ''B_4''B_4$. The CE is the same as that in [20-23], i.e., the cylinder $A_1B_1A_2B_2A_3B_3A_4B_4\ A_1'B_1'A_2'\ B_2'A_3'B_3'A_4'B_4'$. Refer to Fig. 4.1(b). The centroid of the top surface of the CE, i.e., the polygon $A_1B_1A_2B_2A_3B_3A_4B_4$, is used as the solution point, which is denoted by Q^*. All flow variables and their spatial derivatives are solved and stored at these solution points.

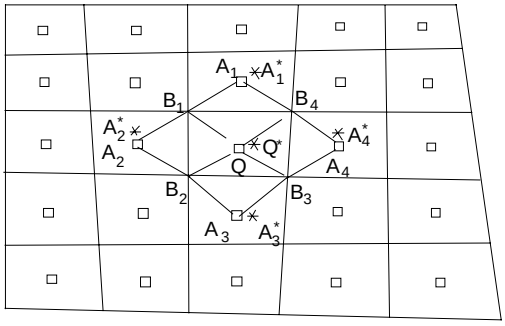

(a)

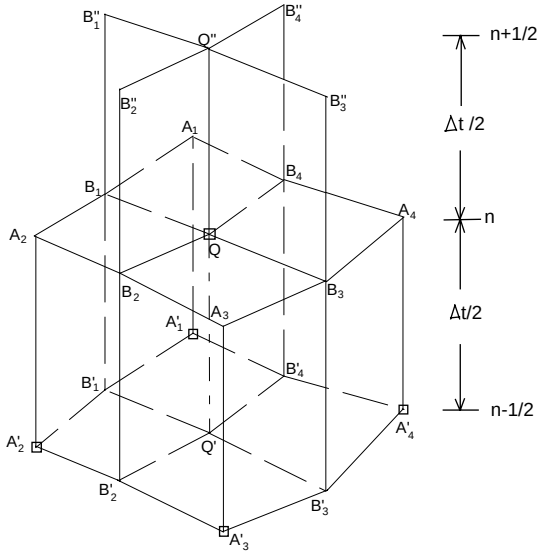

(b)

Fig. 4.1: The space-time geometry of the modified space-time CE/SE method: (a) representative grid points in an x-y plane, (b) the definitions of CE and SE.

Inside each SE, the flow variables are assumed smooth, and the structure of the flow solution is descretized by a prescribed function. Following Chang's approach, the distribution of the flow variables is represented by the first-order Taylor series. For any $(x, y, t) \in$ SE(Q), $u_m(x, y, t)$, $f_m(x, y, t)$ and $g_m(x, y, t)$ are approximated by:

$$u_m^*(x,y,t) = (u_m)_{Q^*} + (u_{mx})_{Q^*}(x - x_{Q^*}) + (u_{my})_{Q^*}(y - y_{Q^*}) + (u_{mt})_{Q^*}(t - t^n) \qquad (4.3a)$$

$$f_m^*(x,y,t) = (f_m)_{Q^*} + (f_{mx})_{Q^*}(x - x_{Q^*}) + (f_{my})_{Q^*}(y - y_{Q^*}) + (f_{mt})_{Q^*}(t - t^n) \quad (4.3b)$$

$$g_m^*(x,y,t) = (g_m)_{Q^*} + (g_{mx})_{Q^*}(x - x_{Q^*}) + (g_{my})_{Q^*}(y - y_{Q^*}) + (g_{mt})_{Q^*}(t - t^n) \quad (4.3c)$$

where x_{Q^*}, y_{Q^*}, and t^n are the space-time coordinates of point Q^*. Accordingly,

$$\vec{h}_m^*(x,y,t) = (f_m^*(x,y,t), g_m^*(x,y,t), u_m^*(x,y,t)) \quad (4.4)$$

Thus, the space-time flux conservation, Eq. (4.2), can be approximated by its discrete counterpart:

$$\oint_{S(CE)} \vec{h}_m^* \cdot ds = \int_{CE} \mu_m dv. \quad (4.5)$$

Substituting Eqs. (4.3) and (4.4) into Eq. (4.5), we obtain the following equation,

$$(u_m)_{Q^*}^n + \frac{\Delta t}{2}\mu (u_m)_{Q^*}^n = (\sum_{l=1}^{4} R_m^{(l)})/S \quad (4.6)$$

where

$$\begin{aligned} R_m^{(l)} &= S_q^{(l)}[(u_m)_{A_l^*}^{n-1/2} + (x_q^{(l)} - x_{A_l^*})(u_{mx})_{A_l^*}^{n-1/2} \\ &\quad + (y_q^{(l)} - y_{A_l^*})(u_{my})_{A_l^*}^{n-1/2}] \\ &+ \sum_{k=1}^{2}\{n_{kx}^{(l)}[(f_m)_{A_l^*}^{n-1/2} + (x_k^{(l)} - x_{A_l^*})(f_{mx})_{A_l^*}^{n-1/2} \\ &\quad + \Delta t/4 \cdot (f_{mt})_{A_l^*}^{n-1/2} + (y_k^{(l)} - y_{A_l^*})(f_{my})_{A_l^*}^{n-1/2}]\} \\ &+ \sum_{k=1}^{2}\{n_{ky}^{(l)}[(g_m)_{A_l^*}^{n-1/2} + (x_k^{(l)} - x_{A_l^*})(g_{mx})_{A_l^*}^{n-1/2} \\ &\quad + \Delta t/4 \cdot (g_{mt})_{A_l^*}^{n-1/2} + (y_k^{(l)} - y_{A_l^*})(g_{my})_{A_l^*}^{n-1/2}]\} \end{aligned} \quad (4.7)$$

for *l=1, 2, 3,* and *4*, indicating the spatial flux contribution from the four neighboring points, and *m=1,2,3,4* and *5*, indicating the five flow equations. Here, $(x_q^{(l)}, y_q^{(l)})$ and $S_q^{(l)}$ for *l*=1, 2, 3 and 4, are the coordinates of centroids and their areas of the four neighboring quadrilaterals $A_1B_1QB_4$, $A_2B_2QB_1$, $A_3B_3QB_2$, and $A_4B_4QB_3$, respectively; $\vec{n}_k^{(l)} = (n_{kx}^{(l)}, n_{ky}^{(l)}, 0)$ and $(x_k^{(l)}, y_k^{(l)}, t^n - \Delta t/4)$ for l = 1, 2, 3, 4 and k = 1, 2, represent the surface vectors and the space-time coordinates of their centroids of the eight lateral boundary surfaces of the CE, i.e., $A_1B_4A_1'B_4'$, $A_1B_1A_1'B_1'$, $A_2B_1A_2'B_1'$, $A_2B_2A_2'B_2'$, $A_3B_2A_3'B_2'$, $A_3B_3A_3'B_3'$, $A_4B_3A_4'B_3'$, $A_4B_4A_4'B_4'$, respectively. Note that the surface vector is defined as the unit outward normal vector (outward from the interior of the CE) multiplied by its area; *S* is the area of the polygon $A_1B_1A_2B_2A_3B_3A_4B_4$, which is also the top surface of the present CE. (Refer to Fig. 4.1)

Due to the source term, Eq. (4.6) is an non-linear equations of $(u_m)_{Q^*}$. Given the values of the marching variables at the $t^{n-1/2}$ time level, the right hand side of (4.6), i.e., (4.7), can be explicitly calculated. To calculate $(u_m)_{Q^*}$ by solving Eq. (4.6), the Newton's method is used. The initial condition for the iterations is calculated by assuming null source term.

To proceed, a central difference type reconstruction approach is employed to calculate $(u_{mx})_{Q^*}$ and $(u_{my})_{Q^*}$. First, according the definition of SEs, we can get the approximated u_m at the four neighbor points A_1^*, A_2^*, A_3^* and A_4^*, by using the Taylor series expansion in time only. By using these u_m and the solution of $(u_m)_{Q^*}$ at point Q^*, we can calculate spatial derivatives $(u_{mx}^{(l)})_{Q^*}$ and $(u_{my}^{(l)})_{Q^*}$, for *l=1, 2, 3,* and *4*, by using the Green-Gauss theory. Finally, by using simple average or re-weighting average, we can obtain the $(u_{mx})_{Q^*}$ and $(u_{my})_{Q^*}$ at point Q^*. Again, details can be found in [20-23]. We remark that the above scheme can be used in unstructured as well as structured meshes.

For the three-dimensional equations, Eq. (2.1), similar approach is adopted. We can get the following equation for $(u_m)_{Q^*}$ at point Q^*:

$$(u_m)_{Q^*}^n + \frac{\Delta t}{2}\mu (u_m)_{Q^*}^n = (\sum_{l=1}^{6} R_m^{(l)})/V \quad (4.8)$$

where

$$\begin{aligned} R_m^{(l)} &= S_q^{(l)}[(u_m)_{A_l^*}^{n-1/2} + (x_q^{(l)} - x_{A_l^*})(u_{mx})_{A_l^*}^{n-1/2} \\ &+ (y_q^{(l)} - y_{A_l^*})(u_{my})_{A_l^*}^{n-1/2} + (z_q^{(l)} - z_{A_l^*})(u_{mz})_{A_l^*}^{n-1/2}] \\ &+ \sum_{k=1}^{4}\{n_{kx}^{(l)}[(f_m)_{A_l^*}^{n-1/2} + (x_k^{(l)} - x_{A_l^*})(f_{mx})_{A_l^*}^{n-1/2} \end{aligned}$$

$$+(y_k^{(l)}-y_{A_i^*})(f_{my})_{A_i^*}^{n-1/2}$$

$$+\Delta t/4\cdot(f_{mt})_{A_i^*}^{n-1/2}+(z_k^{(l)}-z_{A_i^*})(f_{mz})_{A_i^*}^{n-1/2}]\}$$

$$+\sum_{k=1}^{4}\{n_{ky}^{(l)}[(g_m)_{A_i^*}^{n-1/2}+(x_k^{(l)}-x_{A_i^*})(g_{mx})_{A_i^*}^{n-1/2}$$

$$+(y_k^{(l)}-y_{A_i^*})(g_{my})_{A_i^*}^{n-1/2}$$

$$+\Delta t/4\cdot(g_{mt})_{A_i^*}^{n-1/2}+(z_k^{(l)}-z_{A_i^*})(g_{mz})_{A_i^*}^{n-1/2}]\}$$

$$+\sum_{k=1}^{4}\{n_{kz}^{(l)}[(q_m)_{A_i^*}^{n-1/2}+(x_k^{(l)}-x_{A_i^*})(q_{mx})_{A_i^*}^{n-1/2}$$

$$+(y_k^{(l)}-y_{A_i^*})(q_{my})_{A_i^*}^{n-1/2}$$

$$+\Delta t/4\cdot(q_{mt})_{A_i^*}^{n-1/2}+(z_k^{(l)}-z_{A_i^*})(q_{mz})_{A_i^*}^{n-1/2}]\} \quad (4.9)$$

where l =*1, 2, 3, 4, 5,* and *6,* for flux conservation contributed from six neighboring CEs. By solving Eq. (4.8), we can get $(u_m)_{Q^*}$. Similarly, by using the central difference type reconstruction approach, we can get the three spatial derivatives $(u_{mx})_{Q^*}$, $(u_{my})_{Q^*}$ and $(u_{mz})_{Q^*}$ at point Q^*. We refer the interested readers to the cited papers [20-23].

5. Results and Discussions

Here the two- and three-dimensional detonations are calculated using above space-time CE/SE method. The parameters of the flow field are $q_0 = 50$, $E^+ = 50$, $\gamma = 1.2$ and $f = 1.6$. According to the classical theory for detonation instability, the above flow parameters would trigger longitudinal instability. The one-dimensional ZND analytical solution derived in Section 3 is employed as the initial condition for both two- and three- dimensional detonations.

5.1 Two-Dimensional detonation Waves

The width of the computational domain is 7.5 $L_{1/2}$, and the height is 9.0. Fifty-four thousand quads are used for the computational domain. The coordinates are fixed on the detonation front. Periodic boundary conditions are imposed along the two lateral boundaries. The detonation is traveling from bottom to top. The flow conditions on the upper boundary surface are fixed according to the unburned gas. The non-reflective boundary condition is used on the bottom surface. Figure 5.1(a-d) is a snapshot of the mass fraction, pressure, vorticity, and temperature, respectively. The numerical result is plotted twice to enhance the visual interpretation. The flow field in Fig. 5.1 is composed of: (i) the quiescent state of the reactant before the shock, (ii) a von Neumann spike with finite rate reaction, and (iii) the equilibrium state after the reaction zone. Due to the two-dimensional cellular structure of the detonation, the flow field is much more complex. The shock front is characterized by mushroom-shaped incident shocks interacting with a Mach stem. The width of the Mach stem changes in a periodic fashion and tremendous vortices are created during the process. At each collision of triple points, new pair of vortices with opposite rotational directions are created and propagate downstream. Due to these vortices, unburned reactant is engulfed into the flame zone and creating the unburned pockets behind the flame zone. The continuous burning of the unburned pockets behind the flame zone greatly extended the effective flame zone. In general, the flow features shown in Fig. 5.1 are consistent with previous reported numerical and experimental results.

2D Detonation -------- (a) Mass Fraction Contours

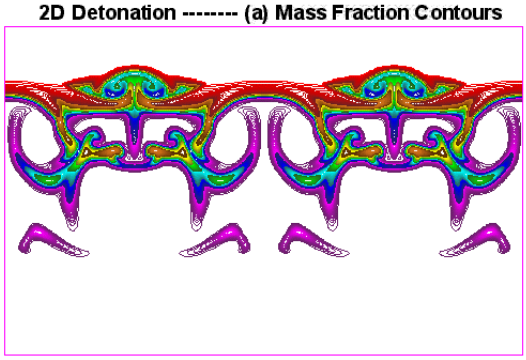

2D Detonation -------- (b) Pressure Contours

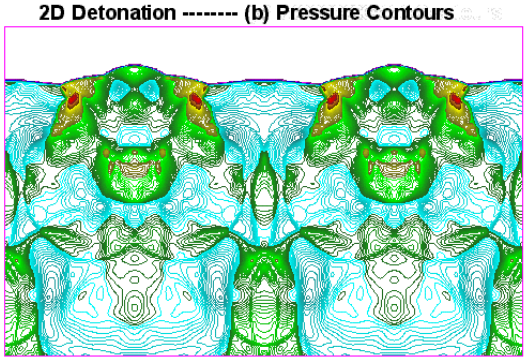

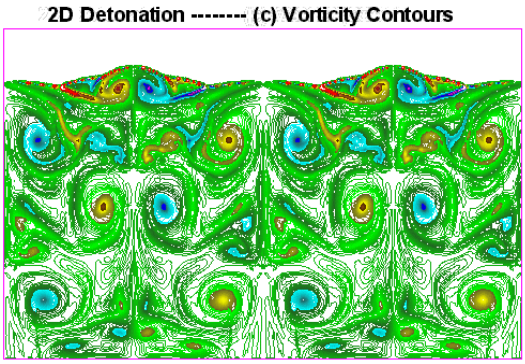

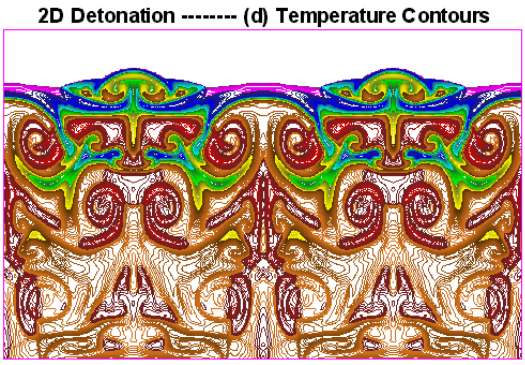

Fig. 5.1 Two-dimensional detonation waves: (a) mass fraction, (b) pressure, (c) vorticity, (d) temperature.

5.2 Detonations in a Tube with Wavy Wall

As shown in Fig. 5.2, the width of the tube is 8 $L_{1/2}$, and the length is 40. The top, bottom and the left boundaries are solid walls. The right boundary is an open outlet. Initially the tube is filled with reactant. The initial detonation wave is located at x=10, a distance from the left boundary. The detonation travels from left to right. Because of flow symmetry, only half of the wavy tube is calculated. About sixty-two thousand quads are used for the computational domain. The reflective boundary condition is imposed along all solid walls. A space-time non-reflective boundary condition is used in the outlet surface. The flow condition is the same as that in Fig. 5.1.

Figure 5.2 shows the pressure and temperature contours at $t = 20$, when the detonation wave just exits the tube outlet. The flow pattern is much more complex than that in a straight tube. Due to the continuous reflection/dispersion of the detonation waves, the traveling speed of the detonation waves in the waving tube is about 10% slower than that in the straight tube. This weaker and slower detonation provide precious time lag to allow ignition and combustion of hydrocarbon fuel, which could be critical for practical use of liquid fuel in a detonation device. Detailed analyses of this flow field will be presented in another paper.

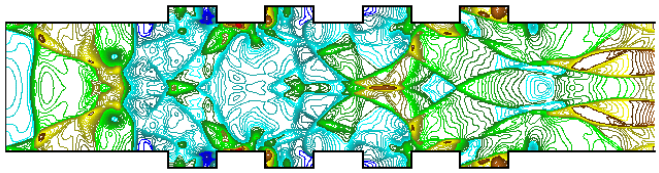

(a)

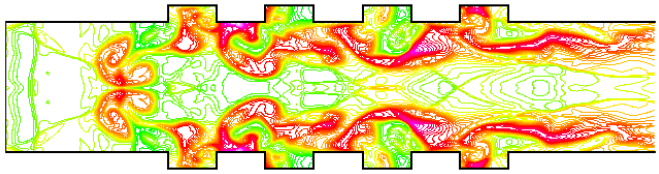

(b)

Fig. 5.2 Detonations travel in a wavy-walled tube: (a) pressure, and (b) temperature.

5.3 Three-Dimensional Detonation Waves

The computation domain is 6×6×6 and 320,000 hexes are used in the computational domain. The analytical ZND solution is employed as the initial condition. The flow conditions are the same as that in Fig. 5.1. The periodic boundary condition is imposed along the four lateral surfaces. The detonation is traveling from bottom to top. Figure 5.3 shows the three-dimensional detonation results. Pressure contours at three different surfaces are shown. The numerical result is plotted twice in both x and y directions to enhance the visual interpretation. This flow pattern in each surface is similar to the two-dimensional one.

If the four lateral boundaries are solid walls, the reflective solid boundary condition is used at the solid walls. Detailed analysis of three-dimensional detonations in a square tube is presented in another paper in the same conference, AIAA 2001–0140. We note that the focal point of the present method is a

new numerical method applied to detonations. The same method is applied to detonations through a tube using a parallel computer with mesh nodes up to 6 millions. In particular, the diagonal instability wave structure is reported in AIAA 2001–0140.

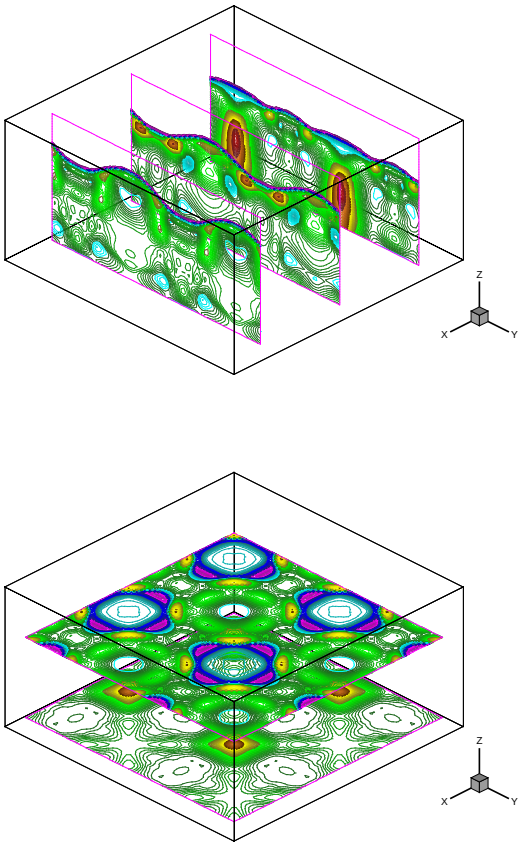

Fig. 5.3 Three-dimensional detonation results of pressure contours at different surfaces.

6. Concluding Remarks

In the present paper, the modified space-time CE/SE method, which is based on using quads and hexes in structured meshes, has been employed to solve the two-and three-dimensional detonations. In this method, only one CE at each grid point is employed to solve two- and three-dimensional flow equations. The spatial gradients of the flow variables are calculated by using a central-differencing reconstruction procedure. This extended CE/SE method maintains all advantageous features of the original CE/SE method with simpler logic and higher computational efficiency.

All salient features of detonations are crisply resolved, including transverse wave structure, triple points, Mach stem, counter rotating vortices, and unburned pockets. The result obtained is consistent with the previous numerical results.

Acknowledgement

This work was performed under the support of NASA Glenn Research Center NCC3-580, and is part of an ongoing program at Wayne State University in applying the Space-Time CE/SE method to practical engineering problems.

References

1. J. H. S. Lee and I. O. Moen, "The Mechanism of Transition from Deflagration to Detonation in Vapor Cloud Explosions," *Prog. Energy Combust. Sci.*, **6**, pp.359-389.
2. W. Fickett and W. W. Wood, "Flow Calculations for Pulsating One-Dimensional Detonations," *Physics of Fluids*, **9,**No.3, pp.903-916, 1966.
3. W. Fickett and W. C. Davis, "Detonation," University of California Press, Berkeley California, (1979).
4. S. Taki and T. Fujiwara, "Numerical Analysis of Two Dimensional Nonsteady Detonations," *AIAA Journal*, **16**, No.1, January 1978.
5. S. Taki and T. Fujiwara, "Numerical Simulation of Triple Shock Behavior of Gaseous Detonation," *Eighteenth Symposium (international) on Combustion, The Combustion Institute*, 1981,pp.1671-1681.
6. V. N. Gamezo, D. Desbordes, and E. S. Oran, "Formation and Evolution of Two-dimensional Cellular Detonations," *Combustion and Flame*, **116**, pp.154-165, 1999.
7. K. Kailasanath, E. S. Oran, J. P. Boris, and T. R. Young, "Determination of Detonation Cell Size and the Role of Transverse Waves in Two-Dimensional Detonations," *Combustion and Flame*, **61,** pp.199-209, 1985.
8. D. N. Williams, L. Bauwens, and E. S. Oran, "Detailed Structure and Propagation of Three-Dimensional Detonations," *Proceedings of the Twenty-Sixth Symposium (International) on Combustion*, The Combustion Institute, pp.2991-2998, 1996.

9. Bourlioux, A. J. Majda, and V. Roytburd, "Theoretical and Numerical Structure for Unstable One-Dimensional Detonations," *SIAM J. Appl. Math*., **51** (1991), pp.303-343.

10. Bourlioux and A. J. Majda, "Theoretical and Numerical Structure of Unstable Detonations," *Phil. Trans. R. Soc. Lond. A*, **350** (1995), pp.29-68.

11. J. J. Quirk, "Godunov-Type Schemes Applied to Detonation Flows," *ICASE Report No.93-15*, also NASA Contractor Report 191447, April 1993.

12. S. Yungster. and K. Radhakrishnan, "A Fully Implicit Time Accurate Method for Hypersonic Combustion: Application to Shock Induced Combustion Instabilities," *NASA TM 106707, also AIAA Paper 94-2965*, 30th Joint Propulsion Conference, Indianapolis, IN, June 1994.

13. M. V. Papalexandris, "Unsplit Numerical Schemes for Hyperbolic Systems of Conservation Laws with Source Terms," Ph.D. Thesis, California Institute of Technology, 1997.

14. D.N. Williams, L Bauwens and E.S. Oran, "Detailed Structure and Propagation of Three-Dimensional Detonations", 26th Symposium on combustion, 2991-2998, 1996.

15. S.C. Chang, X.Y. Wang, and C.Y. Chow, "New Developments in the Method of Space-Time Conservation Element and Solution Element-Applications to Two-Dimensional Time-Marching Problems," *NASA TM 106758*, December 1994.

16. S.C. Chang, "The Method of Space-Time Conservation Element and Solution Element – A New Approach for Solving the Navier Stokes and Euler Equations," *J. Comput. Phys*., **119**, pp.295-324, 1995.

17. S.C. Chang, S.T. Yu, A. Himansu, X.Y. Wang, C.Y. Chow and C.Y. Loh, The Method of Space-Time Conservation Element and Solution Element – A New Paradigm for Numerical Solution of Conservation Laws, *Computational Fluid Dynamics Review*, **1**, 206 (1998), Edited by M. Hafez and K. Oshima, World Scientific Publisher.

18. S.C. Chang, X.Y. Wang and C.Y. Chow, The Space-Time Conservation Element and Solution Element Method: A New High-Resolution and Genuinely Multidimensional Paradigm for Solving Conservation Laws, *J. Comput. Phys.*, **156**, 89 (1999), jcph.1999.6354.

19. X.Y. Wang and S.C. Chang, A 2D Non-Splitting Unstructured Triangular Mesh Euler Solver Based on the Space-Time Conservation Element and Solution Element Method, *Computational Fluid Dynamics Journal*, **8**, 309 (1999).

20. Z.C. Zhang and S.T. Yu, Shock Capturing without Riemann Solver---A Modified Space-Time CE/SE Method for Conservation Laws, AIAA Paper 99-0904.

21. Z.C. Zhang, S.T. Yu, S.C. Chang, A. Himansu and P. Jorgenson, A Modified Space-Time CE/SE Method for Euler and Navier-Stokes Equations, AIAA Paper 99-3277.

22. Z.C. Zhang, S.T. John Yu, X.Y. Wang, S.C. Chang, A. Himansu and P.C.E. Jorgenson, "The CE/SE Method for Navier-Stokes Equations Using Unstructured Meshes for Flows at All Speeds," *AIAA Paper 2000-0393*.

23. Z.C. Zhang, S.T. John Yu, and S.C. Chang, "The Space-Time CE/SE Method for the Euler Equations on Quadrilateral and Hexagonal Meshes," Submitted to *J. Comput. Phys*.

24. S.T. Yu and S.C. Chang, "Treatments of Stiff Source Terms in Conservation Laws by the Method of Space-Time Conservation Element and Solution Element," *AIAA Paper 97-0435*, 35th AIAA Aerospace Sciences Meeting, January 1997, Reno, NV.

25. S.J. Park, S.T. Yu, M.C. Lai, S.C. Chang,and P.C.E. Jorgenson, "Direct Calculations of Stable and Unstable ZND Detonations by the Space-Time CE/SE method," *AIAA Paper 98-3212*, 34th AIAA Joint Propulsion Conference, July 1998, Cleveland, Ohio.

26. S.J. Park, S.T. Yu, M.C. Lai, S.C. Chang,and P.C.E. Jorgenson, "Numerical Calculation of Unstable Detonations by the Space-Time Conservation Element and Solution Element method," *AIAA Paper 99-0491*.